

Anisotropic Superexchange in βMnS †

J. J. PEARSON*

University of Pittsburgh, Pittsburgh, Pennsylvania

(Received November 27, 1961)

The suggestion by Keffer of an anisotropic superexchange of the Moriya type in βMnS led to the present detailed calculation. Whereas Moriya's work was confined to ions with one electron in the $3d$ shell and to cases of low symmetry, this calculation was performed for a half-filled $3d$ shell and tetrahedral symmetry. The unperturbed state was taken to consist of two Mn^{++} ions together with their common S^{--} nearest neighbor, each in a tetrahedral crystal field. The perturbing Hamiltonian contained the electronic spin-orbit interaction and the Coulomb interaction between electrons on neighboring ions. The mechanism involved going from the ground state to an excited crystal field state on one Mn^{++} ion by the spin-orbit effect, then back to the ground state by superexchange between the Mn's. The direction of the \mathbf{D} vector was found to be perpendicular to the plane of the three ions, and its magnitude of the order of a superexchange integral times the spin-orbit parameter over a crystal field splitting energy. The existence of the effect depends importantly upon π overlap between the Mn and S orbitals.

I. INTRODUCTION

It has been shown by Keffer¹ that the existence of an anisotropic superexchange interaction of the form

$$H = \mathbf{D} \cdot \mathbf{S}_1 \times \mathbf{S}_2 \quad (1)$$

between magnetic nearest-neighbor spins in βMnS will resolve a paradox which has long existed in the interpretation of the powder neutron diffraction pattern of that crystal. He observed that the presence of such an interaction, in sufficient magnitude to outweigh the magnetic dipole interaction among the spins, would permit a spin ordering in the crystal which is consistent with the observed diffraction pattern and at the same time minimizes the energy. The purpose of the present calculation was to determine the size and direction of \mathbf{D} in βMnS . Interactions of the form (1) were first suggested on symmetry grounds by Dzyaloshinsky,² but it remained for Moriya³ to propose a detailed mechanism by which they could arise. Moriya's derivation, however, was confined to magnetic ions with only one electron (or hole) in their $3d$ shells, whereas the Mn^{++} ions to be considered here have half-filled d shells. Also, the local symmetry in the present case is tetrahedral, whereas Moriya's work was done for crystals of lower symmetry.

II. THE PRESENT METHOD

The structure of βMnS is the zinc-blende structure.⁴ Each pair of Mn^{++} ions has one common S^{--} nearest neighbor through which superexchange between the two Mn's presumably takes place. This S ion instead of lying on the centerline of the two Mn's is displaced from

† This work was done in the Sarah Mellon Scaife Radiation Laboratory and was supported by the U. S. Air Force through the Air Force Office of Scientific Research of the Air Research and Development Command.

* Present address: Department of Physics, University of California at San Diego.

¹ F. Keffer, preceding paper [Phys. Rev. **126**, 896 (1962)].

² I. Dzyaloshinsky, J. Phys. Chem. Solids **4**, 241 (1958).

³ T. Moriya, Phys. Rev. Letters **4**, 228 (1960); Phys. Rev. **120**, 91 (1960).

⁴ R. W. G. Wyckoff, *Crystal Structures* (Interscience Publishers, Inc., New York, 1960), Vol. 1.

it, the two Mn-S lines making an angle of 109.5° with each other. To avoid ambiguity the coordinates shown in Fig. 1 will be used throughout. Thus the lines to the sulfur from Mn_1 and Mn_2 are in $[111]$ and $[\bar{1}\bar{1}\bar{1}]$ directions, respectively. In this structure the local environment seen by each of the ions is described by the tetrahedral symmetry group T_d . The operations of the group T_d are the same as those of the cubic group without inversion (O) except for the twofold rotations about face diagonals and the fourfold rotations. These elements are replaced in T_d by the corresponding rotations each combined with an inversion, giving classes $6\sigma_d$ and $6S_4$. The character tables of the two groups are identical,⁵ (as are their operations applied to d functions, which have even parity). As can be seen from these tables, there are two threefold representations, one twofold, and two onefold. This symmetry implies a mirror plane passing through the three ion sites being considered, and thus \mathbf{D} is required to be perpendicular to this plane.³

In the free ion, Mn^{++} has five electrons in its $3d$ shell, combining according to Hund's rules to form a 6S ground state. It is therefore necessary to extend the Moriya mechanism to the case of a half-filled d shell. In this calculation the unperturbed states are again taken to be states of the free ions in a crystal field. For the present the only Mn^{++} electronic states to be con-

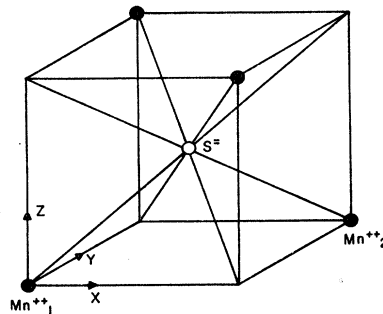


FIG. 1. Ionic arrangement and crystal coordinate system in βMnS .

⁵ H. Eyring, J. Walter, and G. E. Kimball, *Quantum Chemistry* (John Wiley & Sons, Inc., New York).

sidered are those within the spectroscopic configuration d^5 . The central field approximation is assumed, with individual one-particle orbitals combining in Slater determinants to form the antisymmetric many-electron functions required by the Pauli principle. The notation $[\varphi_1\varphi_2\varphi_3\varphi_4\varphi_5]$ implies a normalized Slater determinant of the five one-electron orbitals $\varphi_1 \cdots \varphi_5$. Also, when a representation is used in which the individual electron m_l 's are specified, the m_l values are often used in place of φ_1 , etc. Finally, $m_s = -\frac{1}{2}$ is indicated by a bar over the corresponding orbital label. The absence of a bar implies $m_s = +\frac{1}{2}$.

The method to be used here involves taking the expectation value of the "superexchange Hamiltonian" H_{SE} for a state consisting of the "ground state" ψ_G (in which each ion is separately in its crystal field ground state), corrected to first order in perturbation theory by the spin-orbit interaction H_{SO} . H_{SE} and H_{SO} are given by

$$\begin{aligned} H_{SE} &= \sum_i \left[\left(\frac{p_i^2}{2m} \right) + \sum_g (e^2 Z_g / r_{ig}) \right] + \sum_{i \neq j} (e^2 / r_{ij}); \\ H_{SO} &= \sum_i \xi(r_i) \mathbf{l}_i \cdot \mathbf{S}_i; \end{aligned} \quad (2)$$

where i and j run over the electrons and g over the nuclei in the three-ion system. Schematically, the desired expectation value E has the form

$$\begin{aligned} E &= \langle \psi | H_{SE} | \psi \rangle; \\ \psi &= \psi_G + \sum_{I1} \left(\frac{\langle \psi_{I1} | H_{SO} | \psi_G \rangle}{(E_G - E_{I1})} \right) \psi_{I1} \\ &\quad + \sum_{I2} \left(\frac{\langle \psi_{I2} | H_{SO} | \psi_G \rangle}{(E_G - E_{I2})} \right) \psi_{I2}. \end{aligned} \quad (3)$$

Here $I1$ and $I2$ run over the intermediate states for ions 1 and 2 to be discussed in the next section.

The part of this E' linear in the spin-orbit parameter is:

$$\begin{aligned} E' &= \sum_{I1} \frac{\langle \psi_G | H_{SO} | \psi_{I1} \rangle \langle \psi_{I1} | H_{SE} | \psi_G \rangle + \langle \psi_G | H_{SE} | \psi_{I1} \rangle \langle \psi_{I1} | H_{SO} | \psi_G \rangle}{(E_G - E_{I1})} + \sum_{I2} \\ &= \sum_{I1} \frac{\langle \psi_G | H_{SO} | \psi_{I1} \rangle \langle \psi_{I1} | H_{SE} | \psi_G \rangle}{(E_G - E_{I1})} + \sum_{I2} + \text{complex conjugate}. \end{aligned} \quad (4)$$

The complex conjugate arises from the second term in the first line of the equation because of the fact that the operators involved are Hermitian. The matrix element $\langle \psi_{I1} | H_{SE} | \psi_G \rangle$ is somewhat schematic in that it includes not only the straightforward matrix element between Slater determinant states ψ_{I1} and ψ_G , but also the compound matrix elements via other intermediate states which correspond to the various superexchange mechanisms and actually increase the order of the perturbation theory. This point will be dealt with in detail, and the form of these states given in Sec. VIII.

The calculation divides itself into three parts: (a) determination of the excited states; (b) calculation of the spin-orbit matrix elements from the ground state to these excited states; and (c) consideration of the superexchange processes by which the return to the ground states is accomplished. The calculation actually involves sixteen electrons (five on each Mn^{++} and six in the $S^{--} 3p$ shell), and the states ψ_G , ψ_I are really Slater determinants made up of sixteen one-electron orbitals, not all mutually orthogonal (notably those on different centers). In the spin-orbit matrix elements, however, only the five orbitals on the ion being excited are of importance, and the states will be written just as though they involved only these five orbitals. The additional terms introduced by the presence of the other eleven electrons will be of an order which is higher by an interionic overlap and will be ignored as very small compared to the terms retained. In the case of super-

exchange, however, all sixteen electrons must be discussed.

III. DETERMINATION OF THE INTERMEDIATE STATES

Since neither the crystal field nor the interelectronic Coulomb interaction within the ion is small enough with respect to the other to be taken as a perturbation, the Hamiltonian must be simultaneously diagonalized with respect to both. It will be helpful, however, to consider the two extreme situations where one or the other vanishes.

When the crystal field is ignored, the Coulomb interaction splits the d^5 configuration into terms diagonal with respect to L , S , M_L , and M_S and degenerate with respect to M_L and M_S . In the opposite limit, the electrons are completely uncoupled, and the energy states of the system are determined by the states of an individual electron in the tetrahedral crystal field.

The characters of the T_d classes in the five-dimensional representation (for d electrons) of the full rotation group are 5, -1 , 1, 1, -1 . This representation splits into the two irreducible representations T_1 and E corresponding to a threefold and a twofold degenerate energy level with eigenfunctions $d\epsilon$ and $d\gamma$, respectively. The $d\epsilon$ and $d\gamma$ functions can be taken to be⁶

$$\begin{aligned} d\gamma &: u \sim (3z^2 - r^2)/3, \quad v \sim x^2 - y^2; \\ d\epsilon &: \xi \sim 2yz, \quad \eta \sim 2xz, \quad \zeta \sim 2xy. \end{aligned}$$

⁶ Y. Tanabe and S. Sugano, J. Phys. Soc. Japan 9, 753 (1954).

The energy separation $E_\epsilon - E_\gamma$ is conventionally denoted by^{7,8} $10 Dq$ and is dependent upon the strength of the crystalline field and the form of the radial wave function. In the no-Coulomb limit, then, the relative energies of the d^5 states depends only on the "crystal configuration" $d\epsilon^n d\gamma^{5-n}$ to which they belong. The crystal field strengths actually encountered in materials of this kind are sufficiently small in comparison to the Coulomb interaction so that the ${}^6S(d\epsilon^3 d\gamma^2)$ state is the ground state rather than the ground state ($d\epsilon^5$ or $d\gamma^4 d\epsilon$ depending on the sign of Dq) for the crystal field alone. Clearly this actual ground state, which has symmetry A_1 , has a wave function

$${}^6A_1(\frac{5}{2}) = [210-1-2] = [\xi\eta\zeta uv]. \quad (5)$$

Under the combined influence of the Coulomb interaction and the crystalline field, the good quantum numbers are S , M_s , and Γ , where Γ denotes the transformation properties (row or column of irreducible representation) under the operations of T_d , and the states remain degenerate with respect to M_s . The spin-orbit perturbation can connect to a given state only those different states which differ from it by one in M_s . Consequently, the sextet ground state can be connected only to a quartet state by this interaction, and in particular for vanishing crystal field only the 4P states are so connected. As can be seen from their tetrahedral transformation characters, P states belong to the threefold-degenerate representation T_2 of the group T_d . As the crystal field is applied, the 4P wave functions are mixed only with functions of the same symmetry and spin quantum numbers (such functions are contained also in 4G and 4F), so in the general case one need consider as intermediate states only those of the type 4T_2 .

The 4T_2 wave functions are most easily found using the so-called "strong field" scheme,⁶ which takes as its starting point the case of zero Coulomb field. The Pauli principle and the restriction to $S = \frac{3}{2}$ limit the possible crystal configurations to three ($d\epsilon^4 d\gamma$, $d\epsilon^3 d\gamma^2$, and $d\epsilon^2 d\gamma^3$). For simplicity the states with $M_s = \frac{3}{2}$ are con-

sidered. For these states, the five-electron function must contain one "flipped spin." The Pauli principle requires that this spin belong to a $d\gamma$ orbital in the $d\epsilon^2 d\gamma^3$ configuration and to a $d\epsilon$ orbital for $d\epsilon^4 d\gamma$. The representations contained within each configuration are obtained using the concept of the direct product representation.⁵ The five-electron Slater determinants arising from a given configuration belong to the direct product representation of T_d obtained from the irreducible representations to which the individual one-electron orbitals belong. The entire fivefold direct product for each configuration does not appear, however, since the Pauli principle requires that, when two functions differing only by a pair of interchanged orbitals occur, only the antisymmetric combination be permitted. This difficulty is encountered when several orbitals having the same spin and belonging to the same representation occur in a configuration. Thus, $d\gamma^2$ does not involve $T_1 \times T_1 = T_1 + T_2 + E + A_1$, but only $T_1^2 = T_2$. Which of the four on the right is the correct one is easily determined by applying one or two group operations to a sample function. In this way:

$$T_1^2 = T_2; \quad T_1^3 = A_2; \quad \text{and} \quad E^2 = A_2. \quad (6)$$

From this observation the splitting of each configuration is easily obtained. Thus,

$$\begin{aligned} a: \quad d\epsilon^4 d\gamma &= T_1^3 \times T_1 \times E = T_1 + T_2; \\ b: \quad d\epsilon^3 d\gamma^2 &= T_1^2 \times T_1 \times E^2 + T_1^3 \times E \times E \\ &= T_1 + T_2 + 2E + 2A_2 + 2A_1; \\ c: \quad d\epsilon^2 d\gamma^3 &= T_1^2 \times E^2 \times E = T_1 + T_2. \end{aligned} \quad (7)$$

The indices a , b , and c will henceforth refer to these three configurations.

Each of the configurations then contains one and only one function belonging to each row of the representation T_2 . To obtain the actual functions, consider the wave functions for ${}^4P(M_s = \frac{3}{2}, M_L = 1)$, ${}^4P(\frac{3}{2}, 0)$, and ${}^4P(\frac{3}{2}, -1)$. These may be obtained by methods described in Condon and Shortley.⁹ They are:

$$\begin{aligned} {}^4P(\frac{3}{2}, 1) &= [1/(20)^{\frac{1}{2}}] \{ 2[2\bar{2}0-1-2] + 6^{\frac{1}{2}}[21\bar{1}-1-2] + 6^{\frac{1}{2}}[210\bar{0}-2] + 2[210-1-\bar{1}] \}, \\ {}^4P(\frac{3}{2}, 0) &= [1/(10)^{\frac{1}{2}}] \{ -2[\bar{2}10-1-2] - [2\bar{1}0-1-2] + [210-\bar{1}-2] + 2[210-1-\bar{2}] \}, \\ {}^4P(\frac{3}{2}, -1) &= [-1/(20)^{\frac{1}{2}}] \{ 2[\bar{1}10-1-2] + 6^{\frac{1}{2}}[2\bar{0}0-1-2] + 6^{\frac{1}{2}}[21-\bar{1}-1-2] + 2[210-\bar{2}-2] \}, \end{aligned} \quad (8)$$

or in terms of the $d\epsilon$ and $d\gamma$ functions:

$$\begin{aligned} {}^4P(\frac{3}{2}, 1) &= [1/(20)^{\frac{1}{2}}] \{ (-[\xi\zeta uv\bar{v}] - \sqrt{3}[\xi\zeta u\bar{u}v] + [\eta\zeta\bar{\zeta}uv] + [\xi\bar{\xi}\eta uv] - [\xi\eta\bar{\eta}\zeta u] - \sqrt{3}[\xi\eta\bar{\eta}\zeta v]) \\ &\quad + i(-[\eta\zeta uv\bar{v}] + \sqrt{3}[\eta\zeta u\bar{u}v] - [\xi\zeta\bar{\zeta}uv] - [\xi\eta\bar{\eta}uv] - [\xi\bar{\xi}\eta\zeta u] + \sqrt{3}[\xi\bar{\xi}\eta\zeta v]) \}, \\ {}^4P(\frac{3}{2}, 0) &= [i/(10)^{\frac{1}{2}}] \{ -2[\xi\eta uv\bar{v}] - 2[\xi\eta\zeta\bar{\zeta}u] + [\eta\bar{\eta}\zeta uv] + [\xi\bar{\xi}\zeta uv] \}, \\ {}^4P(\frac{3}{2}, -1) &= \{ (-\sqrt{3}[\xi\zeta u\bar{u}v] - [\xi\zeta uv\bar{v}] + [\xi\bar{\xi}\eta uv] + [\eta\zeta\bar{\zeta}uv] - [\xi\eta\bar{\eta}\zeta u] - \sqrt{3}[\xi\eta\bar{\eta}\zeta v]) \\ &\quad + i(-\sqrt{3}[\eta\zeta u\bar{u}v] + [\eta\zeta uv\bar{v}] + [\xi\eta\bar{\eta}uv] + [\xi\zeta\bar{\zeta}uv] + [\xi\bar{\xi}\eta\zeta u] - \sqrt{3}[\xi\bar{\xi}\eta\zeta v]) \}. \end{aligned} \quad (9)$$

⁷ W. G. Penney and R. Schlapp, Phys. Rev. **41**, 194 (1932).

⁸ R. Finkelstein and J. H. Van Vleck, J. Chem. Phys. **8**, 790 (1940).

⁹ E. U. Condon and G. H. Shortley, *The Theory of Atomic Spectra* (Cambridge University Press, New York, 1957).

To obtain functions which are entirely imaginary, the linear combinations

$${}^4P_x(\frac{3}{2}) \equiv (1/\sqrt{2})[{}^4P(\frac{3}{2}, -1) - {}^4P(\frac{3}{2}, 1)]; \quad {}^4P_y(\frac{3}{2}) \equiv (i/\sqrt{2})[{}^4P(\frac{3}{2}, 1) + {}^4P(\frac{3}{2}, -1)]; \quad {}^4P_z(\frac{3}{2}) \equiv {}^4P(\frac{3}{2}, 0), \quad (10)$$

can be taken (in analogy with the spherical harmonic x , y , and z p functions). The wave functions are:

$$\begin{aligned} {}^4P_x(\frac{3}{2}) &= [i/(10)^{\frac{1}{2}}](-\sqrt{3}[\eta\zeta u\bar{u}v] + [\eta\zeta uv\bar{v}] + [\xi\eta\eta uv] + [\xi\zeta\bar{\zeta} uv] + [\xi\bar{\xi}\eta\zeta u] - \sqrt{3}[\xi\bar{\xi}\eta\zeta v]), \\ {}^4P_y(\frac{3}{2}) &= [i/(10)^{\frac{1}{2}}](-[\xi\zeta uv\bar{v}] - \sqrt{3}[\xi\zeta u\bar{u}v] + [\eta\zeta\bar{\zeta} uv] + [\xi\bar{\xi}\eta uv] - [\xi\eta\bar{\eta}\zeta u] - \sqrt{3}[\xi\eta\bar{\eta}\zeta v]), \\ {}^4P_z(\frac{3}{2}) &= [i/(10)^{\frac{1}{2}}](-2[\xi\eta uv\bar{v}] - 2[\xi\eta\zeta\bar{\zeta} u] + [\eta\bar{\eta}\zeta uv] + [\xi\bar{\xi}\zeta uv]). \end{aligned} \quad (11)$$

Since it is already known that these functions transform as T_2 , and since no group operation can mix crystal configurations, it is clear that the unique (to within a unitary transformation) 4T functions belonging to each configuration must be

$$\begin{aligned} {}^4T_{2x^a}(\frac{3}{2}) &= \frac{1}{2}(\sqrt{3}[\xi\bar{\xi}\eta\zeta v] - [\xi\bar{\xi}\eta\zeta u]), \\ {}^4T_{2y^a}(\frac{3}{2}) &= \frac{1}{2}(\sqrt{3}[\xi\eta\bar{\eta}\zeta v] + [\xi\eta\bar{\eta}\zeta u]), \\ {}^4T_{2z^a}(\frac{3}{2}) &= [\xi\eta\zeta\bar{\zeta} u], \\ {}^4T_{2x^b}(\frac{3}{2}) &= (1/\sqrt{2})([\xi\eta\bar{\eta} uv] + [\xi\zeta\bar{\zeta} uv]), \\ {}^4T_{2y^b}(\frac{3}{2}) &= (1/\sqrt{2})([\eta\zeta\bar{\zeta} uv] + [\xi\bar{\xi}\eta uv]), \\ {}^4T_{2z^b}(\frac{3}{2}) &= (1/\sqrt{2})([\eta\bar{\eta}\zeta uv] + [\xi\bar{\xi}\zeta uv]), \\ {}^4T_{2x^c}(\frac{3}{2}) &= \frac{1}{2}(\sqrt{3}[\eta\zeta u\bar{u}v] - [\eta\zeta uv\bar{v}]), \\ {}^4T_{2y^c}(\frac{3}{2}) &= \frac{1}{2}(\sqrt{3}[\xi\zeta u\bar{u}v] + [\xi\zeta uv\bar{v}]), \\ {}^4T_{2z^c}(\frac{3}{2}) &= [\xi\eta uv\bar{v}]. \end{aligned} \quad (12)$$

The most general intermediate level of interest, then, is threefold degenerate, each of its components being a linear combination of the basic states of the same symmetry, say, T_{2x^a} , T_{2x^b} , and T_{2x^c} for T_{2x} , and similarly for T_{2y} and T_{2z} . Again a , b , and c refer to the configurations. There will be three such levels (labeled by $n=1, 2, 3$) and their wave functions can be written as:

$$\begin{aligned} {}^4T_{2x^n} &= \lambda_n {}^4T_{2x^a} + \mu_n {}^4T_{2x^b} + \nu_n {}^4T_{2x^c}, \\ {}^4T_{2y^n} &= \lambda_n {}^4T_{2y^a} + \mu_n {}^4T_{2y^b} + \nu_n {}^4T_{2y^c}, \\ {}^4T_{2z^n} &= \lambda_n {}^4T_{2z^a} + \mu_n {}^4T_{2z^b} + \nu_n {}^4T_{2z^c}. \end{aligned} \quad (13)$$

This set of functions differs by a unitary transformation from the set obtained by Koide and Pryce¹⁰ and Pappalardo.¹¹ Since the steps leading to these functions are not given in these references, it was thought useful to present them here. The parameters μ_n , ν_n , and λ_n as well as the energy differences ΔE_n from the ground state are obtained by the solution of a 3×3 secular equation. The Hamiltonian to be considered is the sum of the Coulomb interaction and the crystal field. Since S and Γ are good quantum numbers and the Hamiltonian is diagonal and degenerate with respect to M_S and the three components of Γ , only three of the basic states, for example, ${}^4T_{2x^a}(\frac{3}{2})$, ${}^4T_{2x^b}(\frac{3}{2})$, and ${}^4T_{2x^c}(\frac{3}{2})$ need be

considered. The crystal field term is diagonal with matrix elements

$$E_C^a = -10Dq, \quad E_C^b = 0, \quad \text{and} \quad E_C^c = 10Dq. \quad (14)$$

The Coulomb matrix elements can either be calculated by assuming radial wave functions and using the methods of Condon and Shortley,⁹ or they can be expressed in terms of the Racah parameters¹² A , B , and C and, together with Dq , left as variables to be fit by optical measurements of other energy levels. In any event, diagonalization of this matrix gives the energy levels as well as the μ 's, ν 's, and λ 's.

IV. THE SPIN-ORBIT MATRIX ELEMENTS

Now that the states ψ_I have been obtained, it is necessary to construct the matrix elements $\langle \psi_G | H_{SO} | \psi_I \rangle$. At this point the question of the spin quantization direction must be introduced. The unperturbed ground state is degenerate with respect to the spin orientation of ions 1 and 2. For the present, ψ_G will be the state in which $M_{S1} = \frac{5}{2}$ along the direction specified by spherical angles θ , φ and $M_{S2} = \frac{5}{2}$ along θ' , φ' . The dependence of E on θ , φ , θ' , and φ' will be determined and the remaining degeneracy discussed in Sec. VII.

Until now it has been assumed implicitly that both space and spin functions were quantized in the x , y , z crystal field system of coordinates. At this point that assumption must be abandoned. The form given in Sec. III for the states ψ_I is clearly independent of the direction of spin quantization. The ${}^4T(M_S)$ functions merely require that M_S and m_s be quantized along the same direction. However, it is easier to calculate spin-orbit matrix elements when m_l and m_s are quantized in the same direction. Thus it is advantageous to express ${}^6A_1(\frac{5}{2}')$ (where the prime is taken to imply quantization along θ, φ) in terms of the various ${}^6A_1(M_S)$ quantized along the crystal z axis. The same applies to ${}^4T_2(\frac{3}{2}')$ and ${}^4T_2(M_S)$. This can be done in each case by diagonalizing the matrix of S_z in the S, M_S representation. This method determines the relations to within a phase factor which must be kept consistent throughout the problem. The results are:

$$\begin{aligned} {}^6A_1(\frac{5}{2}') &= e^{-5i\varphi} \cos^5(\theta/2) {}^6A_1(\frac{5}{2}) + 5^{\frac{1}{2}} e^{-4i\varphi} \sin(\theta/2) \cos^4(\theta/2) {}^6A_1(\frac{3}{2}) + 10^{\frac{1}{2}} e^{-3i\varphi} \sin^2(\theta/2) \cos^3(\theta/2) {}^6A_1(\frac{1}{2}) \\ &\quad + (10)^{\frac{1}{2}} e^{-2i\varphi} \sin^3(\theta/2) \cos^2(\theta/2) {}^6A_1(-\frac{1}{2}) + 5^{\frac{1}{2}} e^{-i\varphi} \sin^4(\theta/2) \cos(\theta/2) {}^6A_1(-\frac{3}{2}) + \sin^5(\theta/2) {}^6A_1(-\frac{5}{2}); \\ {}^4T_2(\frac{3}{2}') &= -i[e^{-4i\varphi} \cos^3(\theta/2) {}^4T_2(\frac{3}{2}) + 3^{\frac{1}{2}} e^{-3i\varphi} \cos^2(\theta/2) \sin(\theta/2) {}^4T_2(\frac{1}{2}) \\ &\quad + 3^{\frac{1}{2}} e^{-2i\varphi} \cos(\theta/2) \sin^2(\theta/2) {}^4T_2(-\frac{1}{2}) + e^{-i\varphi} \sin^3(\theta/2) {}^4T_2(-\frac{3}{2})]. \end{aligned} \quad (15)$$

¹⁰ S. Koide and M. H. L. Pryce, *Phil. Mag.* **3**, 607 (1958).

¹¹ R. Pappalardo, *J. Chem. Phys.* **31**, 1050 (1959).

¹² G. Racah, *Phys. Rev.* **62**, 438 (1952).

To complete the determination of the matrix elements one needs the spin-orbit elements connecting the various ${}^6A_1(M_S)$ components to those of ${}^4T_{2x}(M_S)$, ${}^4T_{2y}(M_S)$, and ${}^4T_{2z}(M_S)$. They can be calculated by returning to the m_l, m_s representation and using Eqs. (2¹¹b) of Condon and Shortley.⁹ The resulting matrix is given as Table I. In the notation of Koide and Pryce¹⁰ σ_n is defined as

$$\sigma_n = (\zeta/5^{\frac{1}{2}})[\sqrt{2}(\lambda_n + \nu_n) = \mu_n], \quad (16)$$

$$\begin{aligned} & \langle {}^6A_1(\frac{5}{2}) | H_{SO} | {}^4T_{2x}(\frac{3}{2}') \rangle \\ &= \sigma_n \left[-\left(\frac{5}{2}\right)^{\frac{1}{2}} e^{i\varphi} \cos^8(\theta/2) - 3\left(\frac{5}{2}\right)^{\frac{1}{2}} e^{i\varphi} \cos^6(\theta/2) \sin^2(\theta/2) \right. \\ &\quad \left. + \left(\frac{5}{2}\right)^{\frac{1}{2}} e^{-i\varphi} \cos^6(\theta/2) \sin^2(\theta/2) - 3\left(\frac{5}{2}\right)^{\frac{1}{2}} e^{i\varphi} \cos^4(\theta/2) \sin^4(\theta/2) + 3\left(\frac{5}{2}\right)^{\frac{1}{2}} e^{-i\varphi} \cos^4(\theta/2) \sin^4(\theta/2) \right. \\ &\quad \left. - \left(\frac{5}{2}\right)^{\frac{1}{2}} e^{i\varphi} \cos^2(\theta/2) \sin^6(\theta/2) + 3\left(\frac{5}{2}\right)^{\frac{1}{2}} e^{-i\varphi} \cos^2(\theta/2) \sin^6(\theta/2) + \left(\frac{5}{2}\right)^{\frac{1}{2}} \sin^8(\theta/2) \right] \\ &= \left(\frac{5}{2}\right)^{\frac{1}{2}} \sigma_n \left[-e^{i\varphi} \cos^2(\theta/2) + e^{-i\varphi} \sin^2(\theta/2) \right] \left[\cos^2(\theta/2) + \sin^2(\theta/2) \right]^3 \\ &= -\left(\frac{5}{2}\right)^{\frac{1}{2}} \sigma_n \left[\cos^2(\theta/2) e^{i\varphi} - \sin^2(\theta/2) e^{-i\varphi} \right]; \\ & \langle {}^6A_1(\frac{5}{2}') | H_{SO} | {}^4T_{2y}(\frac{3}{2}') \rangle \\ &= i\sigma_n \left[\left(\frac{5}{2}\right)^{\frac{1}{2}} e^{i\varphi} \cos^8(\theta/2) + 3\left(\frac{5}{2}\right)^{\frac{1}{2}} e^{i\varphi} \cos^6(\theta/2) \sin^2(\theta/2) \right. \\ &\quad \left. + \left(\frac{5}{2}\right)^{\frac{1}{2}} e^{-i\varphi} \cos^6(\theta/2) \sin^2(\theta/2) + 3\left(\frac{5}{2}\right)^{\frac{1}{2}} e^{i\varphi} \cos^4(\theta/2) \sin^4(\theta/2) + 3\left(\frac{5}{2}\right)^{\frac{1}{2}} e^{-i\varphi} \cos^4(\theta/2) \sin^4(\theta/2) \right. \\ &\quad \left. + \left(\frac{5}{2}\right)^{\frac{1}{2}} e^{i\varphi} \cos^2(\theta/2) \sin^6(\theta/2) + 3\left(\frac{5}{2}\right)^{\frac{1}{2}} e^{-i\varphi} \cos^2(\theta/2) \sin^6(\theta/2) + \left(\frac{5}{2}\right)^{\frac{1}{2}} e^{-i\varphi} \sin^8(\theta/2) \right] \\ &= i\sigma_n \left(\frac{5}{2}\right)^{\frac{1}{2}} \left[e^{i\varphi} \cos^2(\theta/2) + e^{-i\varphi} \sin^2(\theta/2) \right] \left[\cos^2(\theta/2) + \sin^2(\theta/2) \right]^3 \\ &= i\sigma_n \left(\frac{5}{2}\right)^{\frac{1}{2}} \left[\cos^2(\theta/2) e^{i\varphi} + \sin^2(\theta/2) e^{-i\varphi} \right]; \\ & \langle {}^6A_1(\frac{5}{2}') | H_{SO} | {}^4T_{2z}(\frac{3}{2}') \rangle \\ &= \sigma_n \left[2\left(\frac{5}{2}\right)^{\frac{1}{2}} \cos^7(\theta/2) \sin(\theta/2) + 6\left(\frac{5}{2}\right)^{\frac{1}{2}} \cos^5(\theta/2) \sin^3(\theta/2) \right. \\ &\quad \left. + 3\left(\frac{5}{2}\right)^{\frac{1}{2}} \cos^3(\theta/2) \sin^5(\theta/2) + 2\left(\frac{5}{2}\right)^{\frac{1}{2}} \cos(\theta/2) \sin^7(\theta/2) \right] \\ &= \sigma_n \left(\frac{5}{2}\right)^{\frac{1}{2}} \left[2 \cos(\theta/2) \sin(\theta/2) \right]. \end{aligned} \quad (17)$$

It is of interest to compute the spin-orbit matrix elements for the case considered by Moriya of a single electron going from its ground state g to an excited state i with its spin flipped by means of the interaction $\xi \mathbf{l} \cdot \mathbf{s}$. As mentioned earlier this matrix element can be written

$$\langle g(\frac{1}{2}') | \xi \mathbf{l} \cdot \mathbf{s} | i(-\frac{1}{2}') \rangle = \langle g | \xi \mathbf{l} | i \rangle \langle m_s = \frac{1}{2}' | \mathbf{s} | m_s = -\frac{1}{2}' \rangle = i \langle \frac{1}{2}' | \mathbf{d} \cdot \mathbf{s} | -\frac{1}{2}' \rangle, \quad (18)$$

where d is now a constant, real for i and g nondegenerate. The expression for $|\frac{1}{2}'\rangle$ in terms of α and β , the spin functions quantized in the same system as \mathbf{l} , is obtained as before by diagonalizing s_z ; and $|\frac{1}{2}'\rangle$ is derived from it in correct relative phase by means of the "lowering operator." These expressions are:

$$\begin{aligned} |\frac{1}{2}'\rangle &= \cos(\theta/2) e^{-i\varphi} \alpha + \sin(\theta/2) \beta, \\ |-\frac{1}{2}'\rangle &= i \left[\sin(\theta/2) e^{-i\varphi} \alpha - \cos(\theta/2) \beta \right]. \end{aligned} \quad (19)$$

The above matrix element then is

$$\begin{aligned} & i \langle \frac{1}{2}' | \mathbf{d} \cdot \mathbf{s} | -\frac{1}{2}' \rangle \\ &= -\langle \cos(\theta/2) e^{-i\varphi} \alpha \\ &\quad + \sin(\theta/2) \beta | d_x s_x + d_y s_y + d_z s_z | \sin(\theta/2) e^{-i\varphi} \alpha \\ &\quad \quad \quad - \cos(\theta/2) \beta \rangle \\ &= -(\hbar/2) \{ d_x [2 \sin(\theta/2) \cos(\theta/2)] \\ &\quad + d_x [\sin^2(\theta/2) e^{-i\varphi} - \cos^2(\theta/2) e^{i\varphi}] \\ &\quad + i d_y [\cos^2(\theta/2) e^{i\varphi} + \sin^2(\theta/2) e^{-i\varphi}] \}. \end{aligned} \quad (20)$$

where ζ is the ζ_{3d} of Condon and Shortley's Eq. (471). It will be noted that Table I differs from the matrix given by Koide and Pryce¹⁰ by more than the previously mentioned unitary transformation. Their matrix is incomplete and the parts given are in error (although this error does not affect the results of their paper). The desired matrix elements can now be written down as follows

V. A NOTATION FOR SUPEREXCHANGE CALCULATIONS

Superexchange, like direct exchange, is a manifestation of the fact that, because of the Pauli principle, the Coulomb interaction can give rise to energies dependent on the relative spin orientations of the different electrons in the system. Unlike direct exchange, however, superexchange between the electrons of two magnetic ions involves the presence of an intermediate nonmagnetic ion. The study of this phenomenon, then, is essentially the study of the Hamiltonian matrix elements between Slater determinant states involving electron orbitals on three different centers and, consequently, not necessarily mutually orthogonal. In order to consider these matrix elements in detail one may find it helpful to introduce the following pictorial notation.

For a symmetric Hamiltonian such as that of Eq. (2) the matrix elements between Slater determinant states $u_1 \cdots u_N$ and $v_1 \cdots v_N$ can be written

$$M = \text{const.} \sum_P (-1)^P \int u_1^*(1) \cdots \times u_N^*(N) H P v_1(1) \cdots v_N(N) dx_1 \cdots dx_N, \quad (21)$$

where the permutation operators P permute the coordinates (space and spin) of the electrons. The u 's and v 's, but not the determinants as a whole, are taken to be normalized. In all the cases to be considered the same

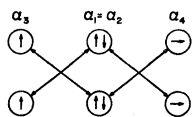


FIG. 2. The Yamashita superexchange mechanism.

set of spatial orbitals will occur in both u and v , although the spins will differ. Let a circle stand for a spatial orbital and an arrow within the circle for the spin function associated with it, two arrows within the circle indicating a doubly occupied orbital. Two directions of quantization, θ, φ and θ', φ' , will be involved, and these will be indicated by vertical and horizontal arrows, respectively. Thus \uparrow and \downarrow will represent states of $m_s = \frac{1}{2}$ and $-\frac{1}{2}$, respectively, along θ, φ , and similarly for \rightarrow and \leftarrow along θ', φ' .

Each term in the sum over P will be represented by a separate diagram with the orbitals u written above the v 's and each spatial orbital in u directly above its counterpart in v . The orbitals centered on ion 1 will be written to the left, those on ion 2 to the right, and those on the S^{--} ion in between. The permutation of the electrons produced by P will be indicated by two-headed arrows joining the position of each electron in u to its position in v . Since H_{SE} is spin independent, the orthogonality of \uparrow and \downarrow causes diagrams with arrows joining the two to vanish; similarly for \rightarrow and \leftarrow . Since H_{SE} is a sum over electrons and pairs of electrons, each diagram implies a sum of integrals in which the one- and two-electron Hamiltonians are allowed to act on the electrons represented by each arrow (or pair of arrows). The matrix element M in turn consists of the sum of all nonzero diagrams. Although the number of diagrams for a given M (particularly with sixteen electrons) is large, in practice only a small number of them (namely those representing large spin-dependent interactions) are of interest.

Clearly, each arrow joining orbitals on different ion sites introduces a factor of the order of magnitude of an interionic overlap into the value of the diagram. It will be assumed, in line with customary procedure, that this factor is zero if the arrow joins sites 1 and 2 (this corresponds to neglecting direct exchange between 1 and 2). Superexchange first appears in terms of fourth order in the overlap, and diagrams of higher order than this are ignored. Also, a diagram will be neglected if it contains an arrow joining two orbitals which are rigorously orthogonal (by virtue of having different azimuthal dependence). These terms are smaller than the others and have been ignored in most previous superexchange calculations. This last approximation will

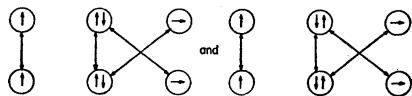


FIG. 3. Cancelling diagrams with doubly-filled orbital.

TABLE I. Matrix elements of spin-orbit interaction connecting the various ground-state components to those of the 4T states.

	${}^4T_{2x^2}(3/2)$	${}^4T_{2x^2}(1/2)$	${}^4T_{2z^2}(-1/2)$	${}^4T_{2z^2}(-3/2)$	${}^4T_{2y^2}(3/2)$	${}^4T_{2y^2}(1/2)$	${}^4T_{2y^2}(-1/2)$	${}^4T_{2z^2}(3/2)$	${}^4T_{2z^2}(1/2)$	${}^4T_{2z^2}(-1/2)$	${}^4T_{2z^2}(3/2)$
${}^6A_1(5/2)$	$-i(5/2)^{1/2}\sigma_n$	0	0	0	$-(5/2)^{1/2}\sigma_n$	0	0	0	0	0	0
${}^6A_1(3/2)$	0	$-i(3/2)^{1/2}\sigma_n$	0	0	0	$-\frac{2}{3}\sigma_n$	0	0	0	0	0
${}^6A_1(1/2)$	$(i/2)\sigma_n$	0	0	0	$-\frac{1}{2}\sigma_n$	0	$-\frac{1}{2}\sqrt{3}\sigma_n$	0	$i\sqrt{3}\sigma_n$	0	0
${}^6A_1(-1/2)$	0	$\frac{1}{2}i\sqrt{3}\sigma_n$	$-(i/2)\sqrt{3}\sigma_n$	0	0	$-\frac{1}{2}\sqrt{3}\sigma_n$	0	0	0	$i\sqrt{3}\sigma_n$	0
${}^6A_1(-3/2)$	0	0	0	$-\frac{1}{2}i\sigma_n$	0	0	$(3/2)^{1/2}\sigma_n$	0	0	0	0
${}^6A_1(-5/2)$	0	0	0	$i(5/2)^{1/2}\sigma_n$	0	0	0	$-(5/2)^{1/2}\sigma_n$	0	0	0

subsequently be referred to as the "orthogonality requirement."

Each diagram corresponds to one of the integrals H_P in the superexchange paper by Keffer and Oguchi¹³ [for example in their Eq. (14)]. As an example of these methods it may be of interest to obtain Eq. (15) of that paper. Consider the diagram shown in Fig. 2 whose value is

$$M = \langle \uparrow | \uparrow \rangle \langle \uparrow | \uparrow \rangle \langle \downarrow | \rightarrow \rangle \langle \rightarrow | \downarrow \rangle$$

$$\times \int \alpha_1(1) \alpha_2(2) \alpha_3(3) \alpha_4(4)$$

$$\times H_{SE} \alpha_1(3) \alpha_2(4) \alpha_3(1) \alpha_4(2) dr_1 \cdots dr_4. \quad (22)$$

The product $|\langle \downarrow | \rightarrow \rangle|^2$ can easily be computed using the known wave functions [Eq. (21)] for $|\downarrow\rangle$ and $|\rightarrow\rangle$.

$$|\langle \downarrow | \rightarrow \rangle|^2 = | \langle i[\sin(\theta/2)e^{-i\varphi}\alpha - \cos(\theta/2)\beta] | \cos(\theta'/2)e^{-i\varphi'}\alpha + \sin(\theta'/2)\beta \rangle |^2$$

$$= | -i[\sin(\theta/2) \cos(\theta'/2)e^{i(\varphi-\varphi')} - \cos(\theta/2) \sin(\theta'/2)] |^2$$

$$= [\sin(\theta/2) \cos(\theta'/2)e^{i(\varphi-\varphi')} - \cos(\theta/2) \sin(\theta'/2)] [\sin(\theta/2) \cos(\theta'/2)e^{-i(\varphi-\varphi')} - \cos(\theta/2) \sin(\theta'/2)]$$

$$= \sin^2(\theta/2) \cos^2(\theta'/2) + \cos^2(\theta/2) \sin^2(\theta'/2) - \sin(\theta/2) \cos(\theta/2) \sin(\theta'/2) \cos(\theta'/2) (e^{i(\varphi-\varphi')} + e^{-i(\varphi-\varphi')})$$

$$= \frac{1}{4} [(1 - \cos\theta)(1 + \cos\theta') + (1 + \cos\theta)(1 - \cos\theta') - 2 \sin\theta \sin\theta' \cos(\varphi - \varphi')]$$

$$= \frac{1}{2} [1 - \cos\theta \cos\theta' - \sin\theta \sin\theta' \cos(\varphi - \varphi')]$$

$$= \frac{1}{2} [1 - \cos((\theta, \varphi), (\theta', \varphi'))]$$

$$= \langle \uparrow | \frac{1}{2}(1 - 4\mathbf{S}_3 \cdot \mathbf{S}_4) | \rightarrow \rangle, \quad (23)$$

or for the spin-dependent part,

$$|\langle \downarrow | \rightarrow \rangle|^2 \sim \langle \uparrow | -2\mathbf{S}_3 \cdot \mathbf{S}_4 | \rightarrow \rangle. \quad (24)$$

It is this product which always occurs to give superexchange. The crossed arrows on the left are necessary also, for with a doubly-filled orbital in the middle, the diagrams in Fig. 3 cancel, as they must since the doubly-filled orbital cannot by itself affect the orientation of another ionic spin. Finally, the energy ΔW of Keffer and Oguchi is obtained by dividing the sum of the two

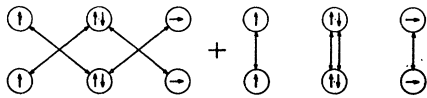


FIG. 4. Diagrams corresponding to matrix elements in ΔW .

diagrams in Fig. 4 by the two terms in the normalization integral in Fig. 5 (where the dashed arrows signify the absence of a Hamiltonian) to obtain

$$\Delta W = \frac{H_I - 2\mathbf{S}_3 \cdot \mathbf{S}_4 H_{13,24}}{1 - 2S^4 \mathbf{S}_3 \cdot \mathbf{S}_4}$$

$$\simeq 2S^4 H_I \mathbf{S}_3 \cdot \mathbf{S}_4 - 2\mathbf{S}_3 \cdot \mathbf{S}_4 H_{13,24}. \quad (25)$$

It is evident that only the diagrams of zeroth order in the overlap S and those of fourth order containing $\mathbf{S}_3 \cdot \mathbf{S}_4$ can enter into the result to fourth order.

Before proceeding to the Moriya case one should note that the above mechanism of superexchange (the

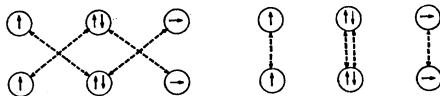


FIG. 5. Normalization integral in ΔW .

¹³ F. Keffer and T. Oguchi, Phys. Rev. **115**, 1428 (1959).

Yamashita mechanism) is not the only one, or even the most important. Other mechanisms involve proceeding through intermediate states in which electrons are transferred from one ion to another, that is by a perturbation process of higher order than first. Two examples of these processes are given by the following diagrams. Here only

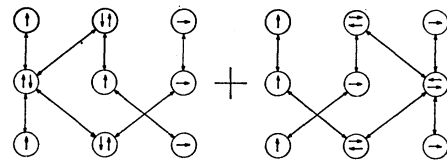


FIG. 6. The Keffer-Oguchi superexchange mechanism.

the matrix elements involving $\mathbf{S}_3 \cdot \mathbf{S}_4$ are indicated. The Keffer-Oguchi mechanism, a second-order perturbation process, can be represented by the diagram in Fig. 6. The Anderson mechanism, involving third-

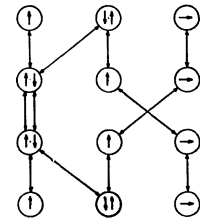


FIG. 7. The Anderson superexchange mechanism.

order perturbation theory, is given by Fig. 7. Both of these examples are seen to be fourth order in the overlap and to involve just the kind of "crossed arrows" found above.

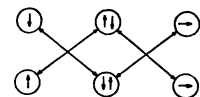


FIG. 8. The Yamashita-type mechanism in anisotropic superexchange.

VI. SOLUTION IN THE MORIYA ONE-ELECTRON CASE

In proceeding to the case of anisotropic superexchange, consider first the one-electron case for which the spin-orbit matrix element was calculated in Sec. V

[Eq. (20)]. Take the Yamashita mechanism as simplest. Then the pertinent diagram for return to the ground state from the excited state is shown in Fig. 8. This involves $H_{13,24}$ as before, but the spin factor is now $\langle \downarrow | \rightarrow \rangle \langle \rightarrow | \uparrow \rangle$. Evaluating this by means of Eq. (19):

$$\begin{aligned}
 & \langle \downarrow | \rightarrow \rangle \langle \rightarrow | \uparrow \rangle \\
 &= \langle i[\sin(\theta/2)e^{-i\varphi\alpha} - \cos(\theta/2)\beta] | \cos(\theta'/2)e^{-i\varphi'\alpha} + \sin(\theta'/2)\beta \rangle \\
 & \quad \times \langle \cos(\theta'/2)e^{-i\varphi'\alpha} + \sin(\theta'/2)\beta | \cos(\theta'/2)e^{-i\varphi\alpha} + \sin(\theta/2)\beta \rangle \\
 &= -i[\sin(\theta/2)\cos(\theta'/2)e^{i(\varphi-\varphi')} - \cos(\theta/2)\sin(\theta'/2)][\cos(\theta'/2)\cos(\theta/2)e^{-i(\varphi-\varphi')} + \sin(\theta'/2)\sin(\theta/2)] \\
 &= -i[\sin(\theta/2)\cos(\theta/2)\cos^2(\theta'/2) - \sin(\theta/2)\cos(\theta/2)\sin^2(\theta'/2) \\
 & \quad + \sin^2(\theta/2)\sin(\theta'/2)\cos(\theta'/2)e^{i(\varphi-\varphi')} - \cos^2(\theta/2)\sin(\theta'/2)\cos(\theta'/2)e^{-i(\varphi-\varphi')}] \\
 &= -i[\frac{1}{2}\sin\theta\cos\theta' - \frac{1}{2}\sin\theta'\cos\theta\cos(\varphi-\varphi') + (i/2)\sin\theta'\sin(\varphi-\varphi')]. \tag{26}
 \end{aligned}$$

No term appears here from the normalization since the numerator has no zeroth-order term. Combining this result with Eq. (20), one can evaluate Eq. (4) in this simple case and obtain:

$$\begin{aligned}
 E' &= \frac{H_{13,24}\hbar}{(E_G - E_{I1})} \text{Re}\{[(i/2)\sin\theta\cos\theta' - (i/2)\sin\theta'\cos\theta\cos(\varphi-\varphi')] \\
 & \quad - \frac{1}{2}\sin\theta'\sin(\varphi-\varphi')\}[-d_x(\cos\theta\cos\varphi + i\sin\varphi) + d_y(i\cos\varphi - \cos\theta\sin\varphi) + d_z\sin\theta] \\
 &= \frac{H_{13,24}\hbar}{(E_G - E_{I1})} \left\{ \frac{1}{2}d_x[\sin\theta\cos\theta'\sin\varphi - \sin\theta'\cos\theta\cos(\varphi-\varphi')\sin\varphi + \sin\theta'\cos\theta\sin(\varphi-\varphi')\cos\varphi] \right. \\
 & \quad \left. + \frac{1}{2}d_y[-\sin\theta\cos\theta'\cos\varphi + \sin\theta'\cos\theta\cos(\varphi-\varphi')\cos\varphi + \sin\theta'\cos\theta\sin(\varphi-\varphi')\sin\varphi] \right. \\
 & \quad \left. - \frac{1}{2}d_z[\sin\theta\sin\theta'\sin(\varphi-\varphi')] \right\} \\
 &= \frac{H_{13,24}\hbar}{2(E_G - E_{I1})} [d_x(\sin\theta\sin\varphi\cos\theta' - \sin\theta'\sin\varphi'\cos\theta) + d_y(\sin\theta'\cos\varphi'\cos\theta - \sin\theta\cos\varphi\cos\theta') \\
 & \quad + d_z(\sin\theta'\sin\varphi'\sin\theta\cos\varphi - \sin\theta\sin\varphi\sin\theta'\cos\varphi')] \\
 &= \frac{2H_{13,24}}{\hbar(E_G - E_{I1})} \langle \uparrow | \mathbf{d} \cdot \mathbf{S}_1 \times \mathbf{S}_2 | \rightarrow \rangle. \tag{27}
 \end{aligned}$$

Again, since θ , φ and θ' , φ' are arbitrary directions, this result indicates that the Hamiltonian is equivalent to

$$\frac{2H_{13,24}}{\hbar(E_G - E_{I1})} \mathbf{d} \cdot \mathbf{S}_1 \times \mathbf{S}_2, \tag{28}$$

as expected from the derivation in Moriya's paper.

VII. THE SIXTEEN-ELECTRON CALCULATION

It is now possible to proceed to the actual problem at hand, for the present confining the calculation to the Yamashita mechanism. Consider each of the orbitals comprising the intermediate-state wave functions $T_{2x,y,z}^n$ to be re-expressed in terms of a coordinate system whose z axis is the line joining the site of Mn_1^{++} to the S^{--} site (a [111] direction in the crystal system) and whose x axis is perpendicular to the plane of the three ions, and the eleven orbitals corresponding to the

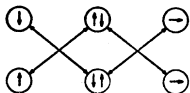


FIG. 9. Possible diagrams for the sixteen-electron case.

ionic ground states of S^{--} and Mn_2^{++} to be included in each Slater determinant. The orbitals on S^{--} are to be expressed as x -, y -, and z -like functions in the same coordinate system as those on Mn_1^{++} , while those on Mn_2^{++} are expressed in a coordinate system whose z axis is along the line $(-1 \ -1 \ 1)$ joining Mn_2^{++} to S^{--} and whose x axis is the same as that in the Mn_1^{++} system.

Consider the possible diagrams representing the return from one of the Slater determinants comprising a T_2^n state to the ground state. Because of the orthogonality requirement each of the p orbitals on S^{--} can have a "crossed-arrow" diagram with only one of the orbitals on Mn_1^{++} (x with xz , y with yz , and z with $3z^2 - r^2$), but with more than one on the Mn_2^{++} (x with xz , y and z with both yz and $3z^2 - r^2$) because of the differing coordinate systems. Hence there are five possible diagrams each having the form shown in Fig. 9, where orbitals whose arrows connect directly below are omitted. These diagrams are specified by the particular orbitals occupying the center and right positions.

Note that the orthogonality requirement forces all the orbitals on the top to be the same as those on the

bottom. This restriction is significant in that it eliminates most of the Slater determinants making up the 4T_2 's. Only three such determinants can give a contribution. They are:

$$[\xi'\eta'\zeta'u'v'], \quad [\xi'\bar{\eta}'\zeta'u'v'], \quad \text{and} \quad [\xi'\eta'\zeta'u'v']. \quad (29)$$

Here the primes on the orbitals indicate that they are of the same form in the new coordinate system as the unprimed orbitals are in the old (that is, $\xi=yz$, $\xi'=y'z'$, etc.). These same restrictions apply in the other superexchange mechanisms to be considered in the next section.

For the calculation of the superexchange matrix elements, then, the functions of Eq. (13) can be expressed in terms of the primed orbitals and only the portions retained which form a linear combination of the determinants of Fig. 9. The same thing can be done in terms of the coordinate system (indicated by double primes) pertinent to Mn_2^{++} for use in the calculations involving states ψI_2 . The relevant transformations are:

$$\begin{aligned} x &= \frac{1}{2}\sqrt{2}[x' + (\frac{1}{3})^{\frac{1}{2}}y' + (\frac{2}{3})^{\frac{1}{2}}z'] \\ &= -\frac{1}{2}\sqrt{2}[x'' + (\frac{1}{3})^{\frac{1}{2}}y'' + (\frac{2}{3})^{\frac{1}{2}}z''], \\ y &= \frac{1}{2}\sqrt{2}[-x' + (\frac{1}{3})^{\frac{1}{2}}y' + (\frac{2}{3})^{\frac{1}{2}}z'] \\ &= -\frac{1}{2}\sqrt{2}[-x'' + (\frac{1}{3})^{\frac{1}{2}}y'' + (\frac{2}{3})^{\frac{1}{2}}z''], \\ z &= [-(\frac{2}{3})^{\frac{1}{2}}y' + (\frac{1}{3})^{\frac{1}{2}}z'] = [-\frac{2}{3}y'' + (\frac{1}{3})z''], \\ u &= [-(\frac{1}{3})^{\frac{1}{2}}v' + (\frac{2}{3})^{\frac{1}{2}}\xi'] = -[(\frac{1}{3})^{\frac{1}{2}}v'' + (\frac{2}{3})^{\frac{1}{2}}\xi''], \\ v &= [(\frac{1}{3})^{\frac{1}{2}}\zeta' + (\frac{2}{3})^{\frac{1}{2}}\eta'] = [(\frac{1}{3})^{\frac{1}{2}}\zeta'' + (\frac{2}{3})^{\frac{1}{2}}\eta''], \\ \zeta &= [(\frac{1}{3})^{\frac{1}{2}}u' - \frac{2}{3}v' + \frac{1}{3}\sqrt{2}\xi'] = [(\frac{1}{3})^{\frac{1}{2}}u'' - \frac{2}{3}v'' + \frac{1}{3}\sqrt{2}\xi''], \\ \eta &= [(\frac{1}{3})^{\frac{1}{2}}u' + \frac{1}{3}v' - (\frac{1}{3})^{\frac{1}{2}}\zeta' + \frac{1}{2}(\frac{2}{3})^{\frac{1}{2}}\eta' - \frac{1}{6}\sqrt{2}\xi'] \\ &= -[(\frac{1}{3})^{\frac{1}{2}}u'' + \frac{1}{3}v'' - (\frac{1}{3})^{\frac{1}{2}}\zeta'' + \frac{1}{2}(\frac{2}{3})^{\frac{1}{2}}\eta'' - \frac{1}{6}\sqrt{2}\xi''], \\ \xi &= [(\frac{1}{3})^{\frac{1}{2}}u' + \frac{1}{3}v' + (\frac{1}{3})^{\frac{1}{2}}\zeta' - \frac{1}{2}(\frac{2}{3})^{\frac{1}{2}}\eta' - \frac{1}{6}\sqrt{2}\xi'] \\ &= -[(\frac{1}{3})^{\frac{1}{2}}u'' + \frac{1}{3}v'' + (\frac{1}{3})^{\frac{1}{2}}\zeta'' - \frac{1}{2}(\frac{2}{3})^{\frac{1}{2}}\eta'' - \frac{1}{6}\sqrt{2}\xi'']. \end{aligned} \quad (30)$$

$$\begin{aligned} E_i' &= 2 \operatorname{Re} \sum_{n=1}^3 [1/(E_G - E_n)] \{ -\sigma_n (\frac{5}{2})^{\frac{1}{2}} (\cos\theta \cos\varphi + i \sin\varphi) [(\lambda_n - \nu_n)/6] \\ &\quad + i \sigma_n (\frac{5}{2})^{\frac{1}{2}} (i \cos\varphi - \cos\theta \sin\varphi) [-(\lambda_n - \nu_n)/6] \} [-\frac{1}{3}H_\xi - (2\sqrt{2}/3)H_u - H_\xi] \\ &\quad \times [(i/2) \sin\theta \cos\theta' - (i/2) \sin\theta' \cos\theta \cos(\varphi - \varphi') - \frac{1}{2} \sin\theta' \sin(\varphi - \varphi')] \\ &= (\frac{1}{3}) (\frac{5}{2})^{\frac{1}{2}} (2H_\xi + \sqrt{2}H_u) \left(\sum_{n=1}^3 \frac{(\lambda_n - \nu_n)\sigma_n}{(E_G - E_n)} \right) [(\sin\theta \sin\varphi \cos\theta' - \sin\theta' \sin\varphi' \cos\theta) \\ &\quad - (\sin\theta' \cos\varphi' \cos\theta - \sin\theta \cos\varphi \cos\theta')] \\ &= \langle \uparrow \rightarrow | \mathbf{D}_1 \cdot \mathbf{S}_1 \times \mathbf{S}_2 | \uparrow \rightarrow \rangle, \end{aligned} \quad (33)$$

where

$$D_{1x} = -(\frac{1}{3}) (\frac{5}{2})^{\frac{1}{2}} (4/25\hbar^2) (2H_\xi + \sqrt{2}H_u) \left(\sum_{n=1}^3 \frac{(\lambda_n - \nu_n)\sigma_n}{(E_G - E_n)} \right) = -D_{1y}. \quad (34)$$

Equation (31) indicates that the terms for states ψI_2 give

$$E_2' = \langle \uparrow \rightarrow | \mathbf{D}_2 \cdot \mathbf{S}_2 \times \mathbf{S}_1 | \uparrow \rightarrow \rangle, \quad (35)$$

where $\mathbf{D}_2 = -\mathbf{D}_1$. Thus

Using these results one finds the significant parts of ${}^4T_{2x}$ and ${}^4T_{2y}$ to be

$$\begin{aligned} {}^4T_{2x} &\rightarrow [(\lambda_n - \nu_n)/6] ([\xi'\eta'\zeta'u'v'] - [\xi'\bar{\eta}'\zeta'u'v']) \\ &= -[(\lambda_n - \nu_n)/6] ([\xi''\eta''\zeta''u''v''] \\ &\quad - [\xi''\bar{\eta}''\zeta''u''v'']), \\ {}^4T_{2y} &\rightarrow -[(\lambda_n - \nu_n)/6] ([\xi'\eta'\zeta'u'v'] - [\xi'\bar{\eta}'\zeta'u'v']) \\ &= +[(\lambda_n - \nu_n)/6] ([\xi''\eta''\zeta''u''v''] \\ &\quad - [\xi''\bar{\eta}''\zeta''u''v'']). \end{aligned} \quad (31)$$

Inspection of the above transformations and of Eq. (12) reveals that ${}^4T_{2x}$ has the same form in both the primed and double-primed representations. This will be seen to lead to its giving no net contribution to the final result.

It will be observed that the absence of the determinant $[\xi'\eta'\zeta'u'v']$ implies a strong dependence of this effect on π overlap. That this overlap can indeed have an appreciable magnitude is shown by Casselman and Keffer.¹⁴ In writing down the integrals corresponding to the remaining diagrams it is helpful to express the function y' on S^- in terms of y'' and z'' . This is done by means of the coordinate transformation shown in Fig. 10 with $\cos\psi = -\frac{1}{3}$. The result is

$$y' = -(\frac{1}{3})(y'' + 2\sqrt{2}z''). \quad (32)$$

The three diagrams of interest are then given in Fig. 11. From Fig. 11 they are seen to occur with coefficients $-\frac{1}{3}$, $-2\sqrt{2}/3$, and 1, respectively. The integrals corresponding to the top and bottom diagrams have the same value. Denote it by H_ξ and that corresponding to the middle diagram by H_u . Finally, the value of E' in Eq. (4) can be calculated in terms of these integrals. In each case the spin part is given by the angular term of Eq. (26).

The part E_1' of E' corresponding to intermediate states ψI_1 is

$$\begin{aligned} E_1' &= E_1' + E_2' = \langle \uparrow \rightarrow | (\mathbf{D}_1 - \mathbf{D}_2) | \uparrow \rightarrow \rangle \\ &= \langle \uparrow \rightarrow | 2\mathbf{D}_1 \cdot \mathbf{S}_1 \times \mathbf{S}_2 | \uparrow \rightarrow \rangle. \end{aligned} \quad (36)$$

¹⁴T. N. Casselman and F. Keffer, Phys. Rev. Letters 4, 498 (1960).

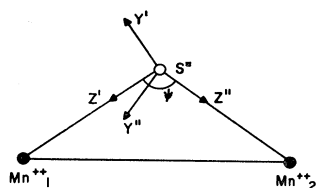


FIG. 10. Coordinate transformation from Mn_1 system to Mn_2 system. (The plane of the paper is the plane of the three ions. The x' , x'' axis is out of the paper.)

It is now possible to see why the T_{2z} terms cannot contribute, since they would give rise to components $D_{1z}=D_{2z}$ which would cancel in the above result. Note that D lies in a $[1\bar{1}0]$ direction, perpendicular to the plane of the three ions as required by the symmetry.

It might seem that this result did not conclusively establish that the spin-dependent part of the energy can be completely expressed in terms of an effective Hamiltonian $\mathbf{D} \cdot \mathbf{S}_1 \times \mathbf{S}_2$ for spins larger than $\frac{1}{2}$, because of the existence of off-diagonal elements of the Hamiltonian connecting different ones of the degenerate states representing different orientations of the ionic ground-state spins. A glance at Fig. 11 reveals, however, that the only states of $S_1=\frac{5}{2}$, $S_2=\frac{5}{2}$ to which the superexchange can return the system from its excited state are the initial state and the three states in which one or both of the Mn^{++} electron spins at the end of a crossed arrow has been flipped. The three new states formed in this way can be taken to be identical to the ionic states $M_{S_1}=\frac{5}{2}$, $M_{S_2}=\frac{3}{2}$; $M_{S_1}=\frac{3}{2}$, $M_{S_2}=\frac{5}{2}$; and $M_{S_1}=\frac{3}{2}$, $M_{S_2}=\frac{3}{2}$ providing these latter states are multiplied by the normalizing factor $(\frac{1}{5})^{\frac{1}{2}}$. This is because, for example, the wave function $M_{S_1}=\frac{3}{2}$ is a sum of five Slater determinants all containing the same spatial orbitals, but each with a different spin flipped, each of these determinants occurring with the same coefficient [hence the factor $(\frac{1}{5})^{\frac{1}{2}}$]. Each of these determinants gives a nonzero contribution to the matrix element only when an arrow joins its flipped spin to the appropriate S^- orbital, and each of these contributions occurs with the same coefficient, establishing the above identity.

Thus the three off-diagonal matrix elements differ only by the factors $(\frac{1}{5})^{\frac{1}{2}}$, $(\frac{1}{5})^{\frac{1}{2}}$, $\frac{1}{5}$ from the corresponding elements in the one-electron case. Since it is known that $\mathbf{d} \cdot \mathbf{s}_1 \times \mathbf{s}_2$ gives all the one-electron elements correctly, it follows that $\mathbf{D} \cdot \mathbf{S}_1 \times \mathbf{S}_2$ gives all the elements in the

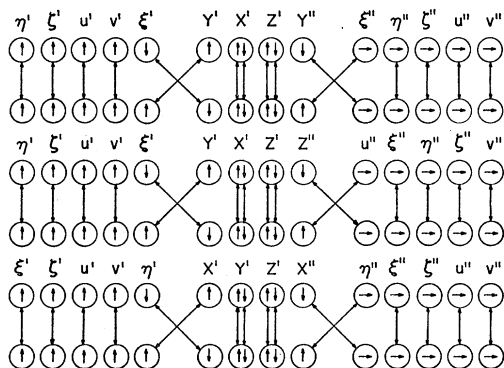


FIG. 11. Diagrams of interest after coordinate transformation.

spin- $\frac{5}{2}$ problem [the numerical factors being given exactly by the difference in factors in front of the raising and lowering operators for spins $\frac{1}{2}$ and $\frac{5}{2}$ in Condon and Shortley's⁹ Eq. (3³3)]. This fact is not surprising, since the most general operator which changes M_{S_1} and M_{S_2} by no more than one unit of angular momentum can be written as a bilinear form in the spin components.

A note may also be appropriate at this point about the peculiar choice of phase factor in Eq. (15). Once it is decided to use the phases implied in Eq. (19) for $|\uparrow\rangle$ and $|\downarrow\rangle$ it becomes imperative to choose the phases in Eq. (15) consistently with them. That this has been done can be seen by noting that Eq. (15) can also be obtained by performing a coordinate rotation (which introduces no phase factors) on the orbitals and transforming the spin functions by means of Eq. (19).

VIII. OTHER SUPEREXCHANGE MECHANISMS

Although the Yamashita mechanism is algebraically simpler, other mechanisms, notably the Anderson mechanism, are probably more important. The Anderson mechanism has one further advantage—that of giving a nonzero result even when the simplifying (if unrealistic) assumption of orthogonal orbitals (zero overlap) is used. Schematically this mechanism is that shown in Fig. 12, as compared with the ordinary superexchange case given in Fig. 7. Notice that no more than two arrows go between different ions in any one matrix element so that a nonzero result is obtained even if the overlap integrals (but not the exchange and transfer integrals, of course) vanish. The angularly dependent spin integrals, $\langle \downarrow | \rightarrow \rangle \langle \rightarrow | \uparrow \rangle$, are the same as before, so the only difference is in the orbital integrals, which are calculated as a straightforward extension of the previous section's work.

The more complicated mechanisms such as this may raise questions concerning the place in the general perturbation scheme of the additional excited states where an electron is transferred from the S^- to an orbital on an Mn^{++} . Such states can, however, be expressed in terms of the unperturbed picture of a free ion placed in a crystal field, although this field no longer has the symmetry T_d . The transfer of the electron reduces the symmetry around both the S^- and the Mn^{++} involved to that of the threefold rotation group C_3 around the axis joining the sites of the two ions. The ionic states of interest must correspond to $S=2$ on the Mn^{++} (at least, by Hund's rules the lowest lying ones must) and to $S=\frac{1}{2}$ on the S^- . These states are degenerate with respect to the Coulomb interaction (since they correspond to $L=2$ on the Mn^{++} and $L=1$ on the S^-) and the Mn states are split by the crystal field into three levels, one of which is made up of the degenerate functions $[\xi\eta\zeta uv\xi]$ and $[\xi\eta\zeta uv\bar{\eta}]$. A similar situation occurs on the S^- , with the two states of interest occurring in a two-dimensional representation, and the new states can be regarded as merely extending the order of the perturbation theory.

IX. NUMERICAL ESTIMATE AND SUMMARY OF RESULTS

It is very difficult to calculate the integrals and energy denominators with any accuracy since the assumption of ordinary atomic wave functions and near-neighbor point-charge crystal fields is known to give answers greatly in disagreement with experiment for problems of this kind. The more accurate use of empirically determined Racah parameters and crystal field strength is impossible because of the lack of optical spectrum data for this crystal. Order-of-magnitude estimates may be made using the optical parameters given by Koide and Pryce¹⁰ for other Mn crystals and the estimates of superexchange integrals by Keffer and Oguchi.¹³ Values of the parameters estimated from these sources are $(2H_t + \sqrt{2}H_u) \sim 10^{-4}$ a.u. and

n	1	2	3
μ_n	0.144	0.597	0.788
ν_n	-0.156	0.801	-0.580
σ_n	228 cm ⁻¹	132 cm ⁻¹	-427 cm ⁻¹
λ_n	0.977	0.040	-0.208
$E_d - E_n$	18950 cm ⁻¹	34200 cm ⁻¹	42700 cm ⁻¹

With these values, Eq. (34) gives a D of the order of 4×10^{-8} a.u.

The purpose of this calculation has been, however, not so much to obtain a numerical result for D , but to demonstrate in detail the existence of a Moriya interaction in this crystal, and, more generally, to outline in detail the mechanism by which such an interaction may take place in crystals with more than one electron in

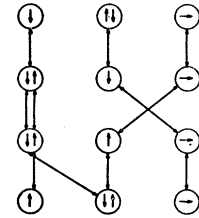


FIG. 12. Anderson's mechanism applied to anisotropic superexchange.

the d shells and with higher symmetry than heretofore considered.

In summary, it has been shown that an anisotropic bilinear interaction of the form $\mathbf{D} \cdot \mathbf{S}_1 \times \mathbf{S}_2$ takes place between the ionic spins of neighboring Mn^{++} ions in βMnS . The mechanism is similar to that proposed by Moriya for the case of ionic spin $\frac{1}{2}$, involving a perturbation process in which one ion is excited by the spin-orbit interaction to a higher crystal-field state, and the return to the ground state is accomplished by means of superexchange between the two ions via the intervening S^{--} . The existence of the interaction has been shown to depend on the anisotropic crystal field (note that for zero crystal field $\lambda_n = \nu_n$ in Eq. (43) and the interaction vanishes) and the existence of π overlap between the Mn^{++} $3d$ electrons and the p electrons on the S^{--} .

ACKNOWLEDGMENT

The author wishes to thank Professor Frederic Keffer, who suggested this problem, for numerous helpful conversations concerning it.